Effect of Hardfacing on the Damping Characteristics of ASTM A516 G70 Steel

Efecto del recargue superficial sobre las características de amortiguamiento del acero ASTM A516 Grado 70

Efeito do revestimento por soldagem nas características de amortecimento do aço ASTM A516 Grau 70

Hussien A. Hilal [1], M. k. A. Razzaq [2], Hamid Al-Abboodi [3], Ahmed T. Fadhil [4], Adnan N. Abood [5], Huiqing Fan [6], Muhammad Samiuddin [7 (*)]

Recibido: 27/01/2026 Aceptado: 30/03/2026

Summary. - This work systematically evaluates the influence of hardfacing on the damping behavior of ASTM A516 Grade 70 steel using AWS EF15, EFeCr-A1, and EFeMn-A electrodes, revealing a clear correlation between microstructural evolution and vibration damping performance. Elemental migration during hardfacing, combined with varying heat input, leads to significant microstructural transformations in the heat-affected zone (HAZ), including martensite formation, recrystallization, and grain growth, particularly for EF15 and EFeCr-A1 electrodes. The normalized microstructure of the base steel disappears after single-layer deposition, while higher heat input associated with double-layer deposition promotes the formation of refined equiaxed grains. Single-layer deposits of EF15 and EFeCr-A1 exhibit fine dendritic structures, whereas double layers develop coarser austenitic morphologies. In contrast, EFeMn-A produces an austenitic matrix with equiaxed grains for both single and double layers. Double-layer deposits show increased hardness due to the formation of electrode-dependent intermetallic compounds. However, the results reveal that an austenitic matrix significantly enhances damping capacity, while the presence of hard intermetallic phases in double-layer deposits reduces damping performance. The results highlight a hardness–damping trade-off that enables optimized electrode and layer selection for vibration- and wear-critical components.

Keywords: *Hardfacing; HAZ; intermetallic compounds; damping capacity.*

(*) Corresponding author.

[1] Student, Ministry of water resource, State commission for operation irrigation and drainage projects (Iraq), Husseinn313husseinn@gmail.com, ORCID iD: https://orcid.org/0009-0002-4648-9457

[2] Student, Kut Technical Institution, Middle Technical University (Iraq), Mortadha_kareem@yahoo.com, ORCID iD: https://orcid.org/0000-0002-9599-5359

[3] Student, Kut Technical Institution, Middle Technical University (Iraq), hamid80_n88@yahoo.com, ORCID iD: https://orcid.org/000-0003-0642-9396

[4] Student, Tigris way construction company (Iraq), Ahth91@yahoo.com, ORCID iD: https://orcid.org/0000-0001-8627-4501

[5] Student, Middle Technical University (Iraq), adnan_naama_59@mtu.edu.iq, ORCID iD: https://orcid.org/0000-0002-3644-2471;

[6] Professor, State Key Laboratory of Solidification Processing, Northwestern Polytechnical University (China), hqfan3@163.com, ORCID iD: https://orcid.org/0000-0002-1405-9279

[7] Professor, NED University of Engineering and Technology (Pakistan), engr.sami@neduet.edu.pk, ORCID iD: https://orcid.org/0000-0002-2350-6114;

Memoria Investigaciones en Ingeniería, núm. 30 (2026). pp. 177-188
https://doi.org/10.36561/ING.30.12
ISSN 2301-1092 • ISSN (en línea) 2301-1106 – Universidad de Montevideo, Uruguay

Resumen. - *Este trabajo evalúa de manera sistemática la influencia del recargue superficial en el comportamiento de amortiguamiento del acero ASTM A516 Grado 70 utilizando electrodos AWS EF15, EFeCr-A1 y EFeMn-A, estableciendo una correlación directa entre la evolución microestructural inducida por el proceso y el desempeño en la atenuación de vibraciones. La migración de elementos durante el recargue, junto con el aporte térmico aplicado, provoca transformaciones microestructurales significativas en la zona afectada por el calor (ZAC), como formación de martensita, recristalización y crecimiento de grano, especialmente en los casos de EF15 y EFeCr-A1. La microestructura normalizada del acero base desaparece tras la deposición de una sola capa, mientras que el mayor aporte térmico asociado a dos capas favorece la formación de granos equiaxiales refinados. Los depósitos de una sola capa con EF15 y EFeCr-A1 presentan estructuras dendríticas finas, mientras que el electrodo EFeMn-A genera una matriz austenítica con granos equiaxiales en ambas configuraciones. Las dobles capas muestran mayor dureza debido a la formación de compuestos intermetálicos. Sin embargo, una matriz austenítica mejora el amortiguamiento, mientras que las fases intermetálicas duras lo reducen, evidenciando un compromiso entre dureza y capacidad de amortiguamiento.*

Palabras clave: *Recargue superficial; zona afectada por el calor (ZAC); compuestos intermetálicos; capacidad de amortiguamiento.*

Resumo *.* ***-*** *Este trabalho avalia de forma sistemática a influência do revestimento por soldagem (hardfacing) nas características de amortecimento do aço ASTM A516 Grau 70, utilizando os eletrodos AWS EF15, EFeCr-A1 e EFeMn-A, estabelecendo uma correlação direta entre a evolução microestrutural induzida pelo processo e o desempenho na absorção de vibrações. A migração de elementos durante a deposição, associada à energia térmica aplicada, provoca transformações microestruturais significativas na zona afetada pelo calor (ZAC), como formação de martensita, recristalização e crescimento de grão, especialmente para EF15 e EFeCr-A1. A microestrutura normalizada do aço base desaparece após a deposição de uma única camada, enquanto o maior aporte térmico de duas camadas favorece a formação de grãos equiaxiais refinados. Depósitos de camada única com EF15 e EFeCr-A1 apresentam estruturas dendríticas finas, enquanto o eletrodo EFeMn-A gera uma matriz austenítica com grãos equiaxiais em ambas as configurações. Depósitos duplos apresentam maior dureza devido à formação de compostos intermetálicos. Entretanto, a matriz austenítica melhora o amortecimento, enquanto fases intermetálicas duras o reduzem, evidenciando um compromisso entre dureza e capacidade de amortecimento.*

Palavras-chave: *Revestimento por soldagem; zona afetada pelo calor (ZAC); compostos intermetálicos; capacidade de amortecimento.*

1. Introduction. - Hardfacing (HF) has been widely applied in many industries. It involves the process of depositing a tougher material on a matrix and is mainly used to increase component life or on tools that are encounter significant abrasive wear [1-5]. A. P. Wu [6] recorded a reduction in the residual tensile stress in the HF layer. Local post-heating of base metal (BM) surface can influentially lower residual tensile stress if there is an austenitic stainless steel interlayer between the carbon steel and Stellite HF layer. A. H. Jones [7] studied the use of HF coatings for ground-engaging applications. Hardfacing alloys, which can be applied to tools as slurry and then sintered, are improved by the addition of hard powder materials. Tungsten carbide powders of varying sizes were added. The relationship between the particle size of the powder and the size of the abrasive particles was assessed, and an increase in wear resistance was determined. Y. Zhou [8] investigated the influence of Ti additives on a hypoeutectic high chromium cast iron arc surface layer. The results indicated that Ti increases hardness and also makes it more uniform across the depth. M. Leitner [9] assessed the wear and fatigue resistance of arc-welded HF layers for structural steel applications. Mild steel was employed, and metal-cored and solid wires were used as filler metals for the HF. Results showed a reduction in wear of 64% and 69% with flux-cored wire and solid wire, respectively. B. Singh [10] investigated slip damping in layered and joint-welded cantilever structures using a finite-element approach. It has been confirmed that the damping capacity of layered and joint structures can be significantly improved by using tack welds instead of continuous welds. A. A. Ahmad Asoor [11] studied the difference in damping capacity for welded and threaded bolts and nut joints. The results indicated that threaded joints could sustain higher damping than welded joints. M. S. Sani [12] evaluated resistance spot welding used for joining AISI 1010 mild steel and AISI 304 stainless steel sheets. The results showed that discrepancies in natural frequency between FEA and experimental model analysis are less. This research was conducted to study the effect of surface hardening of the fan blades of rotary liner using different electrodes on damping behavior and microstructure of ASTM A516 G70 steel.

2. Experimental Work. - ASTM A516 Grade 70 steel plates with a thickness of 10 mm were used as the substrate material. Hardfacing was carried out using three different surfacing electrodes: AWS EFe15, EFeCr-A1, and EFeMn-A. The chemical compositions of substrate and electrodes are provided in Table 1.

Element	C	Cr	Ni	Mn	Si	P	S	Mo	Nb	Fe
A516 G70	0.12	0.0163	0.0035	1.33	0.323	0.0124	0.0019	0.0072	-	Bal.
EFe15	3.4	22	-	-	-	-	-	-	10	Bal.
EFeCr-A1	2.5	33	-	-	-	-	-	-	-	Bal.
EFeMn-A	0.7	-	3	14	0.1	-	-	-	-	Bal.

Table I. Chemical composition of the substrate and electrodes (wt.%)

Hardfacing was performed using a manual metal arc welding process (MMAW) with electrodes of 3.2 mm diameter. Welding current (120 A), voltage (20 V), and travel speed (2–5 mm/s) were applied. For multilayer deposition, interpass temperatures of 150 °C and bead overlap of 30–50% are commonly applied. The use of double layers introduces additional thermal cycles due to reheating of underlying layer, leading to cumulative heat exposure and associated microstructural modifications, which reasonably explain the observed changes in damping behavior. Seven steel plates were cut with dimensions of 350 × 250 mm and secured in a specially designed fixture to minimize distortion during welding. Hardfacing layers with an approximate thickness of 3 mm were deposited using the back-step technique without preheating. The welding pass width was slightly greater than 40 mm, and welding was conducted in the longitudinal direction with continuously overlapping passes. To evaluate the effect of hardfacing on mechanical and dynamic behavior, both single- and double-layer deposits were produced for each electrode type.

Vibration damping capacity tests were conducted on both as-received and hardfaced specimens with dimensions of 140 × 10 × 4.5 mm. Free vibration decay tests were conducted to evaluate the damping characteristics of hardfaced ASTM A516 G70 steel specimens. The excitation was applied as an initial transverse displacement at free end, followed by release without external forcing. The specimens were tested under cantilever boundary conditions, where one end was rigidly clamped using a steel fixture with a controlled tightening torque (~25–30 N·m) to minimize slippage and fixture compliance effects. The vibration response was measured using a piezoelectric accelerometer

mounted near the free end to capture maximum amplitude. Data acquisition was performed at a sampling rate of 10 kHz. A low-pass filter was applied to reduce high-frequency noise, and signal processing included standard windowing. The logarithmic decrement (δ) was calculated using successive peak amplitudes according to:

$$\delta = \frac{1}{n} \ln \left(\frac{x_1}{x_{n+1}} \right)$$

where n = 5-8 cycles were used for improved accuracy. Peak-picking was carried out using an automated routine in MATLAB. The damping ratio (ζ) was derived from δ using standard relations, and each measurement was repeated three times to ensure repeatability, with averaged values reported.

Microstructural characterization was carried out using optical microscopy (OM), scanning electron microscopy (SEM), Energy Dispersive X-ray Spectroscopy (EDS), and X-Ray Diffraction (XRD). Prior to examination, samples were prepared by standard grinding and polishing procedures. The substrate was etched using a Nital solution, while the hardfaced layers were etched using a chemical solution consisting of 3 parts HCl, 2 parts HNO_3, and 2 parts acetic acid. Microhardness measurements were performed using a load of 300g and a dwell time of 15s. The spacing between adjacent indents was maintained at a constant distance of (1 mm) to avoid interaction between plastic zones. Multiple traverses (three parallel lines) were performed across the weld cross-section to ensure reproducibility. Fusion line (FL) and HAZ boundaries were identified based on OM observations, considering both microstructural changes and etching contrast differences between the base metal, HAZ, and fusion zone (FZ). Furthermore, the reported microhardness profiles represent the average values obtained from multiple traverses, with individual measurements showing good consistency.

3. Results and Discussion. -

3.1 Microstructure analysis. - The microstructure of ASTM A516 G70 steel comprises ferrite and pearlite, with an average grain size of 27µm (Figure I). In a single layer deposited with electrode EFe15, fine niobium carbide (NbC) with an intermetallic compound of chromium silicon ($CrSi_2$) is presented within an austenite matrix, while martensite appears in HAZ (Figure IIA). In double layers, niobium carbide is also existence in the austenite matrix, along with iron carbide precipitated (Fe_5C_2), chromium iron carbide (Cr, Fe)$_7C_3$, and existing martensite in HAZ (Figure IIB). The matrix is a dendritic structure with Dendritic Arm Spacing (DAS) of 7.79µm for a single layer and 9.25µm for double layers.

EDS line confirms that migration of Nb, Cr, and carbon (wt%) from the surface layers to steel increased martensite formation in HAZ (Figs. III and IV). Chromium diffused up to 200µm (with a single layer) in steel, with a sharp gradient in concentration. Niobium diffused with a slight gradient and a penetration depth greater than 400µm. Carbon content significantly increases near FL, which is associated with iron reduction and encourages carbide formation. For double-surface layers, chromium has a lower concentration at the steel side for a penetration depth greater than 400µm. The concentration of alloying elements increases in comparison to a single layer, which reflects an increased hardness. For a single layer, NbC and $CrSi_2$ were present, whereas, in double layers, three different phases were present; NbC, Fe_5C_2, and (Cr, Fe)$_7C_3$, these results were confirmed by XRD analysis (Figure V). This is caused by a longer migration time of elements with an increase in concentration compared to a single layer.

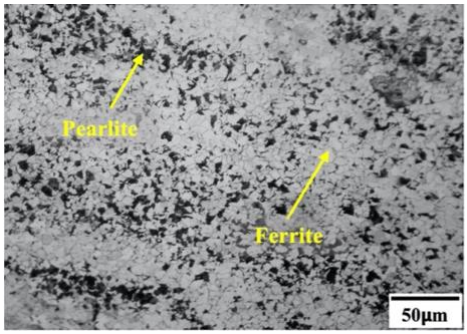

Figure I. Microstructures of ASTM A516 G70

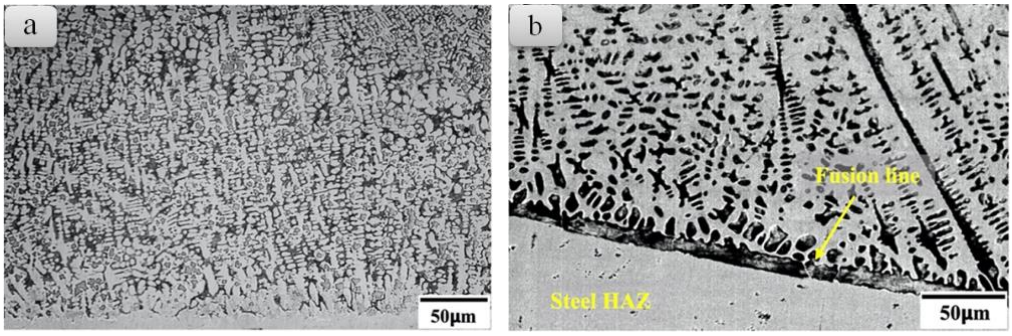

Figure II. (a) Microstructure of HF (a) single layer, (b) double layers using EFe15

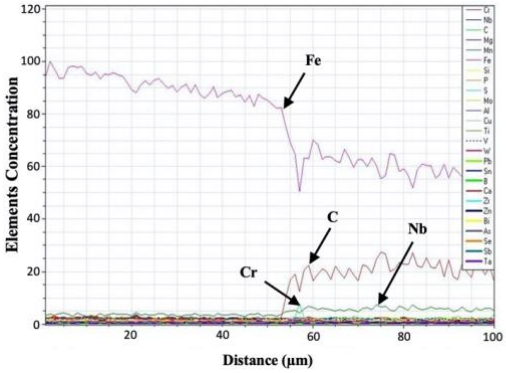

Figure III. Distribution of elements using EFe15 single layer

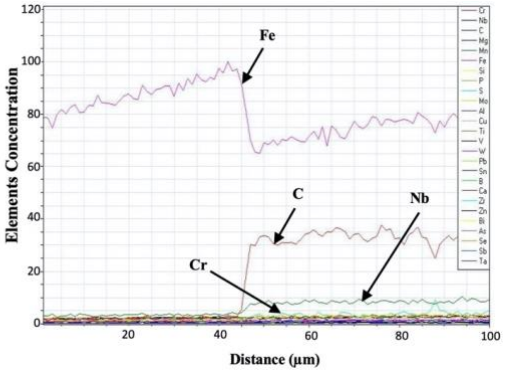

Figure IV. Distribution of elements using EFe15 double layer

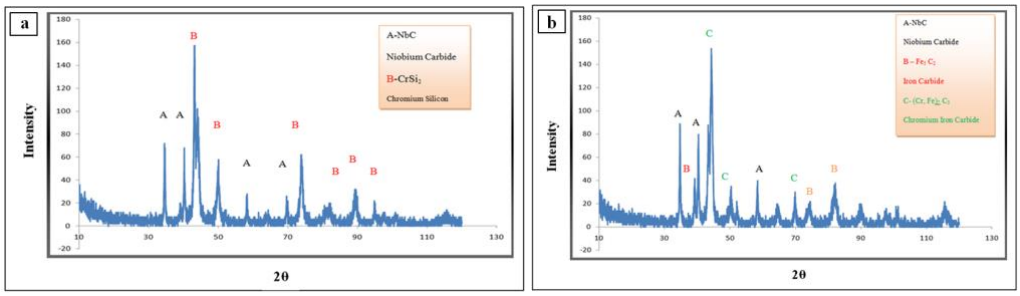

Figure V. XRD of (a) single layer, and (b) double layer using EFe15.

The hardness of A516 G70 steel is improved with a single layer with EFe15. Hardness was raised from 175HV to 450HV on surface (Figure VI). This change in hardness could be related to martensite and carbide formation and the hardness increased to 650HV with double layers owing to the creation of carbides – Fe_5C_2 and $(Cr, Fe)_7C_3$ – associated with the disappearance of $CrSi_2$.

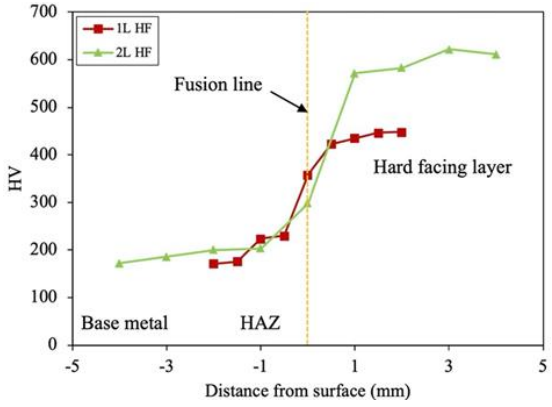

Figure VI. Vickers hardness for single and double layers using EFe15

A single layer of electrode EFeCr-A1 is associated with secondary chromium carbide (Cr_7C_3) in surfacing layer and martensite in HAZ of steel due to the high chromium percentage (Figs.VII and VIII). Double layers recorded same phases mentioned with additional heating without significant effect and migration time on intermetallic compound forming types. With EFeCr-A1 For single and double layers, Fe, Cr and C diffuse from surfacing layer to BM with same profile (Figs. IX and X), but more effectively with double layers. Diffusion regime of Fe (wt%) resembles that of EFe15, especially their increment and sudden reduction near FZ. The carbon concentration increases in double-surface layers along with an increase in the volume fraction of carbides. For single layer; new carbides, Cr_7C_3 is existing, while double layers register that the predominant intermetallic compound is FeCr, with only trace amounts of chromium carbide, these findings are supported by XRD results (Figure XI). Surfacing with a single layer has a more significant effect on hardness, making it greater than 800HV. Using this electrode, however, there was no significant difference in hardness between single and double layers (Figure XII).

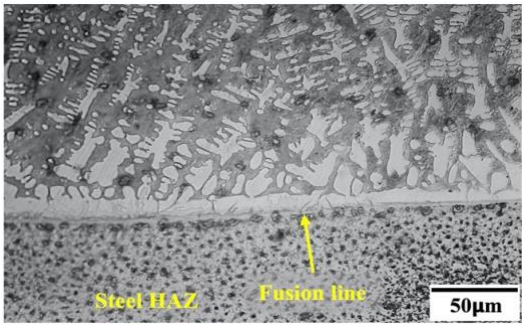

Figure VII. Microstructure of HF single layer using EFeCr-A1

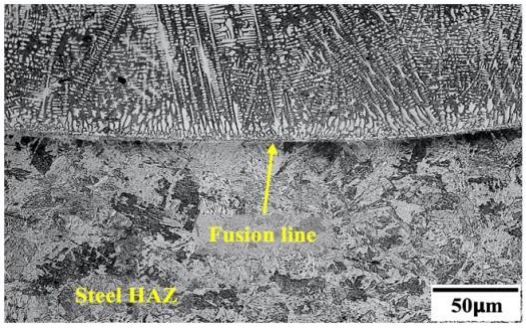

Figure VIII. Microstructure of HF double layers using EFeCr-A1

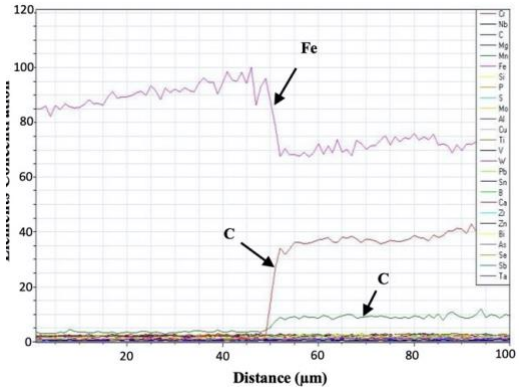

Figure IX. Distribution of elements using EFeCr-A1single layer

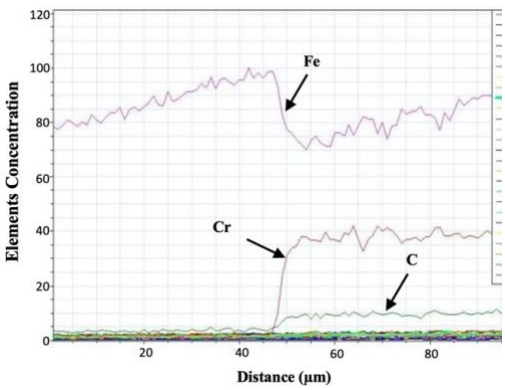

Figure X. Distribution of elements using EFeCr-A1 double layer

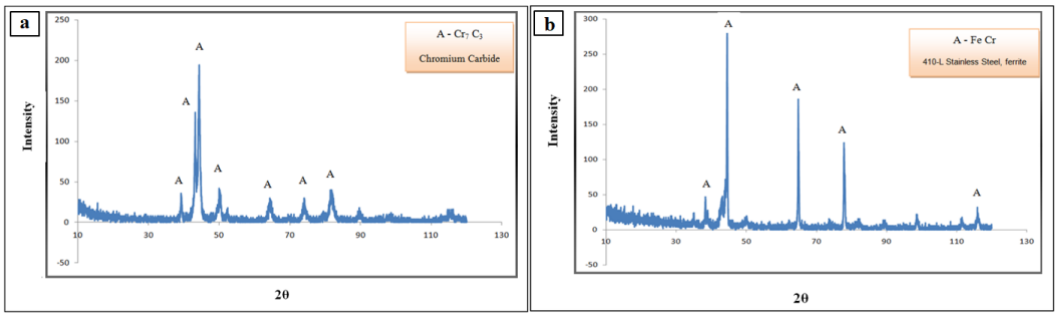

Figure XI. XRD of (a) Single Layer, and (b) double layer using EFeCr-A1

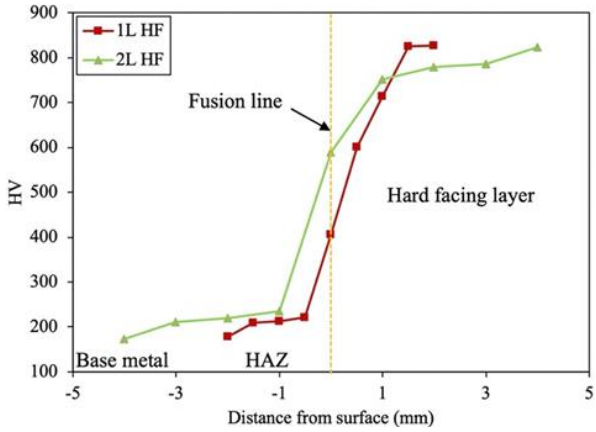

Figure. XII; Vickers hardness with one and double layers HF using EFeCr-A1

One layer with EFeMn-A electrode, austenitic with equiaxed structures is evident. For double layers, manganese carbide (Mn_7C_3) prevails, which is consistent with a study by D. M. Mattox [13]. Steel does not have martensite near FL, but this phenomenon manifests with double layers at depths of 100µm (Figs. XIII and XIV). Variation with a single layer in Fe sharply reduced at a distance of 1.5mm approximately from FL, which is associated with an increase in carbon content, while manganese gradually reduced across FL. Double layer experience increased element concentration, with random variation to some extent. Further, manganese diffuses inside steel and is soluble without forming intermetallic compounds (Figs. XV and XVI). XRD analysis of the single-layer sample revealed two distinct phases (CFe15.1 and Cr–Ni–Fe–C), whereas the double-layer sample exhibited a single phase (Mn_7C_3) (Figure XVII).

Hardness attained more than 800HV at the surface layer. Chromium carbide in HF layers is profit high hardness. Carbon steel having a high thermal conductivity, so HAZ had been formed in different distinct zones, each one having properties differ with another, so will have different hardness values. High heat input encourages the carbon migration toward FL and formation band of martensite near it. Away from FL, the hardness vigorously decreases. This fluctuation related to the transition of microstructures from full martensitic to bainitic until reach unaffected base metal. An increase in hardness was recorded near FL from the steel side for a single layer, with not more than 245HV hardness, while the surface layer registered about 200HV. This makes it clear that the refining zone does not consist of martensite; however, with double layers, the hardness is increased to greater than 300HV, with martensite present near FZ (Figure XIV).

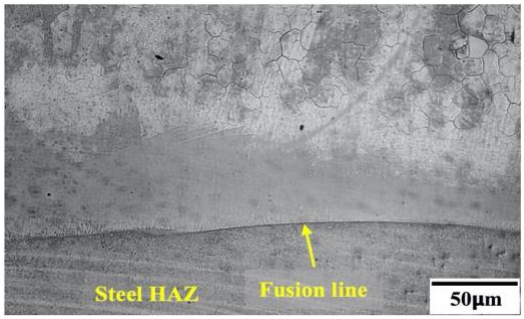

Figure XIII. Microstructure of HF single layer using EFeMn-A

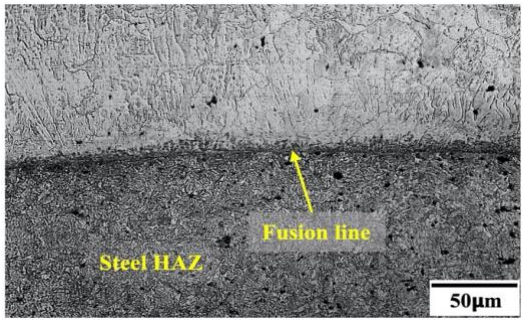

Figure XIV. Microstructure of HF double layer using EFeMn-A

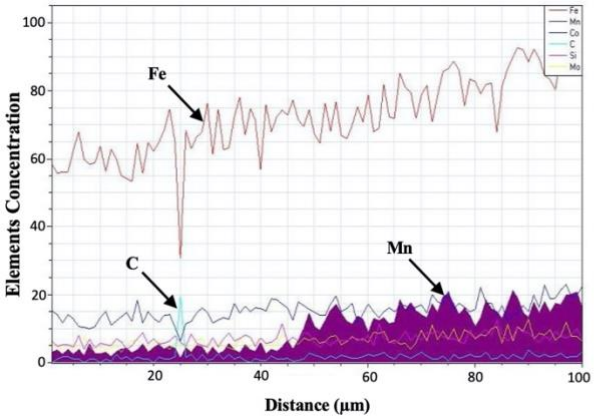

Figure XV. Distribution of elements using EFeMn-A single layer

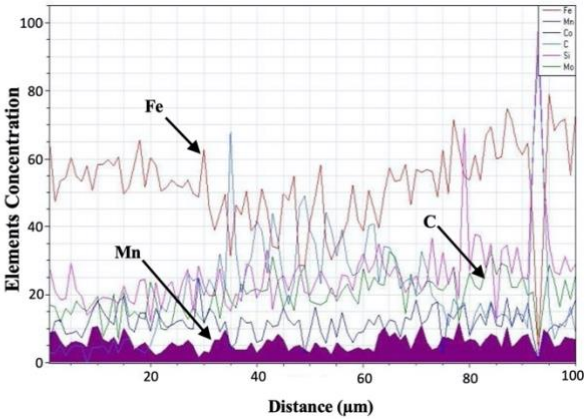

Figure XVI. Distribution of elements using EFeMn-A double layer

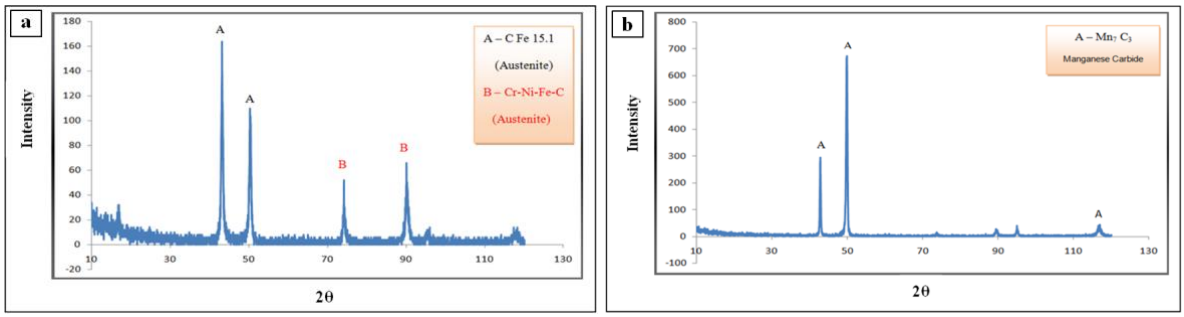

Figure XVII. XRD of (a) single layer, and (b) double layer using EFeMn-A

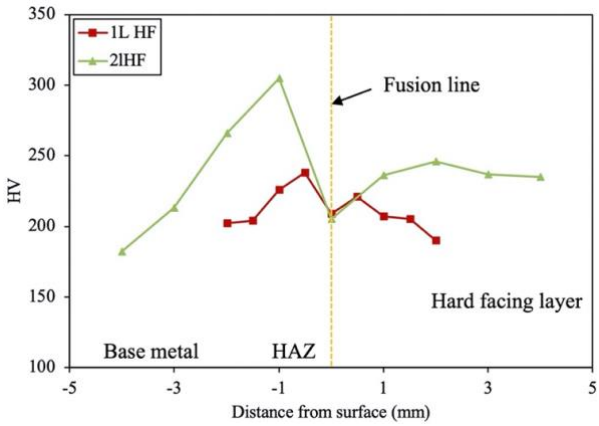

Figure XVIII. Vickers hardness one- and two-layers HF with using EFeMn-A

3.2 Damping Test. - The experimental results of damping test regarding free-vibration response tests implemented in this work are presented. Damping characteristics are represented in terms of logarithmic decrements, damping ratio, and damping capacity, which are shown in Table (II). It can be seen that damping characteristics improved in comparison to as-received steel owing to the contribution of HF materials. In addition, the damping improvement for one layer is higher than that for two layers, for all types of electrodes (Figs. XIX, XX, and XXI). Moreover, the maximum improvement was realized with one layer of EFeMn-A. In general, this development is dependent on the presence of an austenite matrix, and the reduction with double layers is related to the formation of other intermetallic compounds. The creation of Fe_5C_2 and $(Cr, Fe)_7C_3$, along with the disappearance of $CrSi_2$ when using EFe15 lead to reducing damping capacity. While double layers when employing EFeCr-A1, the formation of FeCr instead of Cr_7C_3 subjects damping capacity to a decline. Double layers, using EFeMn-A, are associated with the establishment of Mn_7C_3, which reduces damping also.

Hard Facing Parameters	Damping Capacity (ψ)	Percentage of Improvement
ASTM A516 G70	0.01027	------
One-layer HF using EFeCr-A1	0.01584	54%
Two layers HF using EFeCr-A1	0.01099	7%
One-layer HF using EFe15	0.02518	145%
Two layers HF using EFe15	0.02193	113%
One-layer HF using EFeMn-A	0.03234	214%
Two layers HF using EFeMn-A	0.02774	170%

Table II. Damping ratio of HF with single and double layers

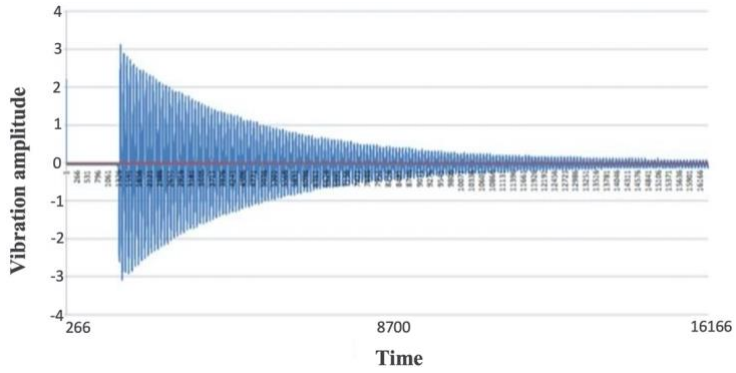

Figure XIX. Free vibration response of ASTM A516 G70

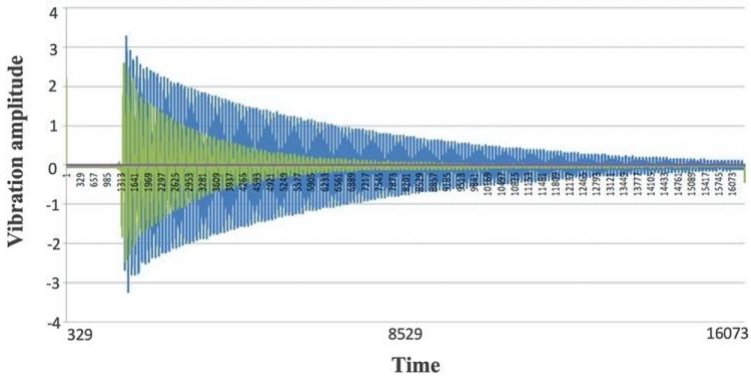

Figure XX. Free vibration response for double layers using EFeCr-A1

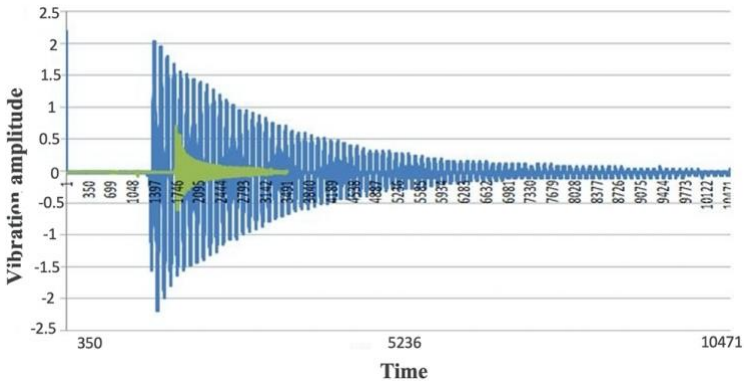

Figure XXI. Free vibration response for double layers using EFeMn-A

4. Conclusions. -

- The heat input associated with hardfacing significantly influences the microstructural evolution of ASTM A516 Grade 70 steel, transforming the normalized microstructure into a heat-affected zone (HAZ) characterized by inhomogeneous grain size distribution.

- Elemental migration across FL occurs for both single- and double-layer hardfacing deposits and follows a broadly similar trend, indicating that layer number has a limited influence on the diffusion regime.

- The presence of an austenitic matrix within the hardfaced layers plays a key role in enhancing the damping capacity of ASTM A516 Grade 70 steel, with the most pronounced improvement observed for single-layer deposits.

- Among the investigated electrodes, single-layer hardfacing using the EFeMn-A electrode exhibits the greatest enhancement in damping capacity, highlighting its suitability for vibration-sensitive applications.

- The application of double-layer hardfacing leads to a reduction in damping capacity for all three electrodes, which is attributed to the formation of brittle intermetallic compounds that restrict energy dissipation during vibration.

References

[1] H. V. Naik1, V. D. Kalyankar, “Development of NiCrSiBC Weld Hardfacing Approach for P91 Steels Used in Steam Turbine Components”, Soldagem & Inspeção. 2021, Vol. 26, 2608-2623.
[2] M. F. Buchely, J. C. Gutierrez, L. M. Le´on, A. Toro, "The effect of microstructure on abrasive wear of hardfacing alloys", Wear, Vol. 259, (2005): pp. 52–61.
[3] X. Wang, F. Hanb, X. Liu , Shiyao Qua, Z. Zoua, "Microstructure and wear properties of the Fe–Ti–V–Mo–C hardfacing alloy", Wear, Vol. 265, (2008): pp. 583–589.
[4] B. Venkatesh, K. Sriker, and V. S. V. Prabhakar. "Wear characteristics of hardfacing alloys: state-of-the-art." Procedia Materials Science, Vol.2, No.10, (2015): pp. 527-532.
[5] J. Brezinová , D. Draganovská, A. Guzanová, P. Balog and J. Vi ˇ náš, "Influence of the Hardfacing Welds Structure on Their Wear Resistance", Metals, Vol. 6, No. 36,(2016): pp. 1-12.
[6] A. P. Wu, J. L. Ren, Z. S. Peng, H. Murakawa, and Y. Ueda. "Numerical simulation for the residual stresses of Stellite hard-facing on carbon steel." Journal of materials processing technology, Vol.101, No. 1 (2000): pp. 70-75.
[7] Jones, Alan Hywel, P. Roffey. "The improvement of hard facing coatings for ground engaging applications by the addition of tungsten carbide." Wear, Vol.267, No. 5-8 (2009): pp. 925-933.
[8] Zhou, Yefei, Yulin Yang, Jian Yang, Feifei Hao, Da Li, Xuejun Ren, and Qingxiang Yang. "Effect of Ti additive on (Cr, Fe) $_7C_3$ carbide in arc surfacing layer and its refined mechanism", Applied Surface Science, Vol. 258, No. 17 (2012): pp.6653- 6659.
[9] Leitner, Martin, Philip Pichler, Florian Steinwender, and Christoph Guster. "Wear and fatigue resistance of mild steel components reinforced by arc welded hard layers." Surface and Coatings Technology, Vol.2, No.330 (2017): pp.140-148.
[10] Singh, B., and B. K. Nanda. "Mechanism of Damping in Welded Structures using Finite Element Approach." World Academy of Science, Engineering and Technology, Vol.4, No. 3 (2010): pp. 771-775.
[11] A. A. Asoor, Ahmadi, M. H. Pashaei. "Experimentally study on the effects of type of joint on damping." World applied sciences journal, Vol. 8, No. 5 (2010): pp. 608- 613.
[12] Sani, M. S. M., N. A. Nazri, and D. A. J. Alawi. "Vibration analysis of resistance spot welding joint for dissimilar plate structure mild steel 1010 and stainless steel 304)." In IOP Conference Series: Materials Science and Engineering, Vol. 238, No. 1 (2017).
[13] D. M. Mattox. "Surface effects on the growth, adhesion and properties of reactively deposited hard coatings". Surface and Coatings Technology, Vol. 81, No. 1, (1996), pp.8-1

Author contribution:
1. Conception and design of the study
2. Data acquisition
3. Data analysis
4. Discussion of the results
5. Writing of the manuscript
6. Approval of the last version of the manuscript

HAH has contributed to: 1, 2, 4, and 5.
MKA has contributed to: 2, and 3.
HAA has contributed to: 2.
ANA has contributed to: 3, and 4.
HF has contributed to: 6.
MS has contributed to: 4, 5, and 6.

Acceptance Note: This article was approved by the journal editors Dr. Rafael Sotelo and Mag. Ing. Fernando A. Hernández Gobertti.